

Structure–property effects in the generation of transient aqueous benzoic acid anhydrides by carbodiimide fuels

Lasith S. Kariyawasam, Julie C. Kron, Run Jiang, André J. Sommer, and C. Scott Hartley*

Miami University, Department of Chemistry & Biochemistry, Oxford, Ohio 45056, United States

E-mail: scott.hartley@miamioh.edu

Abstract

The design of dissipative systems, which operate out-of-equilibrium by consuming chemical fuels, is challenging. As yet, there are few examples of privileged fuel chemistries that can be broadly applied in abiotic systems in the same way that ATP hydrolysis is exploited throughout biochemistry. The key issue is that designing nonequilibrium systems is inherently about balancing the relative rates of coupled reactions. The use of carbodiimides as fuels to generate transient aqueous carboxylic anhydrides has recently been used in examples of new nonequilibrium materials and supramolecular assemblies. Here, we explore the kinetics of formation and decomposition of a series of benzoic anhydrides generated from the corresponding acids and EDC under typical conditions (EDC = *N*-(3-dimethylaminopropyl)-*N'*-ethylcarbodiimide hydrochloride). The reactions can be described by a simple mechanism that merges known behavior for the two processes independently. Structure–property effects in these systems are dominated by differences in anhydride decomposition rate. The kinetic parameters

allow trends in concentration-dependent properties to be simulated, such as reaction lifetimes, peak anhydride concentrations, and yields. For key properties there are diminishing returns with the addition of increasing amounts of fuel. These results should provide useful guidelines for the design of functional systems making use of this chemistry.

Introduction

An important characteristic of many biochemical processes is that they require energy input to provide function or maintain their state.¹ Such processes are referred to as “dissipative”.^{2,3} Species formed by dissipative self-assembly can exhibit behavior such as spatiotemporal control, self-replication, self-healing, and adaptivity that are not possible at thermodynamic equilibrium.³⁻⁵ However, chemically fueled dissipative systems remain rare outside of biology. Examples include molecular hydrogels with time-dependent mechanical properties and unique fiber (dis)assembly dynamics;⁶⁻¹¹ aggregates as transient nanoreactors and coatings;^{12,13} ion transport channels for active or gated transport;^{14,15} molecular motors;¹⁶ hosts for catch-and-release binding;^{17,18} and controlled block copolymer assemblies.^{19,20}

Recently, Boekhoven²¹⁻²⁵ and our group^{26,27} have used carbodiimides to fuel the formation of transient aqueous anhydrides from carboxylic acid precursors. The context of this chemistry (nonequilibrium assembly) is modern, but the reactions themselves have been long known: the overall process is just carboxylate-catalyzed hydration of the carbodiimide.²⁸ The anhydrides, commonly invoked as intermediates in carbodiimide coupling reactions,²⁹ are essentially byproducts that happen to incorporate the key unstable covalent bond. Importantly, the carbodiimide fuel is not incorporated into the nonequilibrium state and thus does not directly impact its function. This behavior contrasts with that of other fuels, such as methylating agents,⁷ which donate structural components to the transient state. That is, the carbodiimide-fueled system begins at equilibrium ($\text{acid} \rightleftharpoons \text{anhydride}$) and is driven away from its equilibrium concentrations, rather than reaction with the fuel producing some

new species that did not previously exist, even in principle.³⁰ While simple, this property enables new behavior, such as intramolecular bond formation.^{21,24,26}

Designing systems for equilibrium self-assembly focuses on well-understood thermodynamic parameters and tends to make use of a relatively small number of well-vetted reactions that can be broadly applied in different systems (e.g., hydrogen bonding, dynamic covalent chemistry). These reactions are typically high-yielding and fast; at least naively, their details can be ignored so long as the desired product is energetically favored and the chemistry reversible. In contrast, designing dissipative systems that make use of transient bonding is inherently challenging because it requires tuning reaction rates.³¹ A set of generally applicable chemical fuel reactions for the formation of transient bonds does not yet exist, although the value of a small number of well-characterized reactions is suggested by the ubiquity of ATP hydrolysis in biochemistry.

To be widely used, a fuel reaction for non-equilibrium systems chemistry would have to make use of a commercially available, cheap fuel; operate on simple, easily incorporated functional groups; and be experimentally straightforward and tunable. We believe that carbodiimide-fueled anhydride formation has the potential to be such a go-to tool. Before designing new systems making use of these reactions, however, it is necessary to understand the effects of changes in substrate structure. The two individual reactions making up this system, the reactions of carbodiimides with carboxylic acids^{28,29,32–43} and anhydride hydrolysis,^{44–54} have been extensively studied in organic chemistry for many decades, but were typically studied separately. Thus, there is little data available that can be used directly to predict behavior in new out-of-equilibrium systems.

Here, we explore on the chemistry of carbodiimide-fueled anhydride formation independent of coupled self-assembly or other processes. Our goal is to explore structure–property effects relevant to dissipative assembly, such as transient state lifetimes. We focus on the reactions of simple benzoic acid derivatives **Ac1–Ac4**, shown in Chart 1, with the common carbodiimide reagent EDC (*N*-(3-dimethylaminopropyl)-*N'*-ethylcarbodiimide hydrochloride).

corresponding urea EDU, and a transient species (presumably **An2**) is formed that reverts to the original acid over time. However, the time scale is inconveniently slow (days) and significant quantities (roughly 30%) of two byproducts are produced. These byproducts comprise both **Ac2**- and EDC-derived moieties and are presumably the isomeric *N*-acylureas formed by unproductive rearrangements of the expected *O*-acylisourea intermediate.^{36,43,58,59} Previous work had shown that a catalytic amount of pyridine minimizes the formation of these byproducts.²⁶ For this work, most reactions were carried out in pyridine/pyridinium buffer, which both eliminated the byproducts and shortened the total reaction times to tens of minutes.⁴²

This chemistry is now reasonably well-precedented;²¹⁻²⁷ however, care was taken to confirm that the transient species observed in the reactions were indeed the corresponding anhydrides. Because **An1** undergoes the slowest hydrolysis (see below), it was possible to independently synthesize it under anhydrous conditions (DCC/CCl₄) and compare its ¹³C{¹H} NMR spectrum⁶⁰ to that of the transient species in D₂O. The spectra match to within 0.1 ppm for each signal. IR spectroscopy was also carried out for all four systems, albeit in unbuffered water to minimize background peaks from the pyridine/pyridinium. As shown in the Supporting Information, a band near 1800 cm⁻¹ was observed in all cases, characteristic of the symmetric stretching modes of the anhydrides.

The four systems were then examined quantitatively by ¹H NMR spectroscopy in D₂O, which allowed the concentrations of all key species to be determined as a function of time (acids, anhydrides, EDC, and EDU). The pD was maintained at 4.5 using the deuterated pyridine/pyridinium buffer system (500 mM). Ionic strengths *I* were kept constant with added NaCl (1.0 M). These conditions were chosen to represent a reasonable baseline method for this chemistry, although variations in pD and buffer concentration were briefly explored. Both concentrations and chemical shifts were determined relative to an internal standard, *N,N*-dimethylacetamide.

Representative ¹H NMR spectra for a typical experiment for the **Ac2/An2** system are

shown in Figure 1. The aromatic ^1H signals of both **Ac2** and **An2** are clearly distinguishable; the EDC and EDU signals are also distinguishable in the aliphatic region of the spectrum (not shown). Early on, the signal for **An2** grows in with a concurrent decrease in **Ac2**, but hydrolysis becomes dominant after a few minutes. Examination of Figure 1 shows that although the chemical shifts of **Ac2** are nearly⁶¹ constant over the course of the experiment, those of **An2** drift; similar behavior was observed for **An1**, **An3**, and **An4**. The chemical shifts are correlated with concentration, suggesting that the anhydrides undergo aggregation into dimers⁶² under the experimental conditions.⁶³ For **An2** and **An4** it was possible to extract data of sufficient quality that dimerization constants K_d could be estimated. They are small in both cases (10 ± 2 and $36 \pm 13 \text{ M}^{-1}$, respectively), indicating that the majority of the anhydride molecules are unassociated even at the highest concentrations achieved in this study. Even were dimerization to completely suppress hydrolysis, the effect on relative rates would be small compared to the overall substituent effects discussed below. Thus, the influence of aggregation was ignored for our analysis.

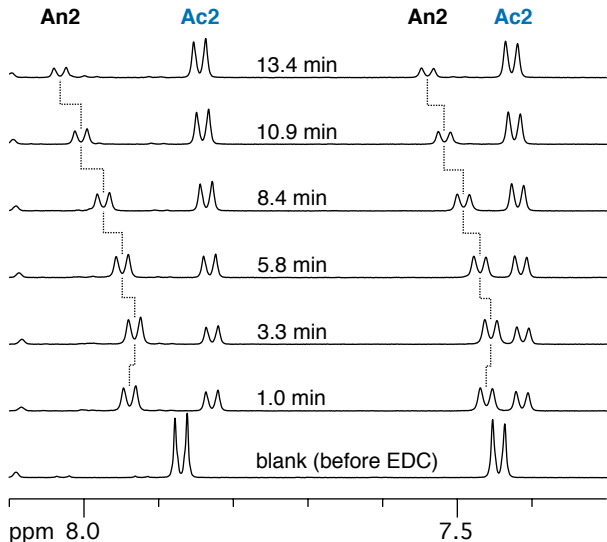


Figure 1: ^1H NMR spectroscopy of **An2** formation on treatment of **Ac2** (45 mM) with EDC (0.75 equiv) (0.5 M pyridine- d_5 buffer, pD 4.5, $I = 1.0 \text{ M}$ (NaCl), D_2O , 298 K).

We expect the initial reaction of the acids with the EDC to generate an acylpyridinium intermediate via the *O*-acylisourea.^{36,40,41} This mechanism is consistent with the observation

that the pyridine buffer suppresses the formation of *N*-acylurea byproducts in the present system and others,⁴² and also with the long history of pyridine-based catalysts (e.g., DMAP) in carbodiimide-mediated reactions.⁶⁴ Similarly, it is very well known that anhydride hydrolysis is catalyzed by pyridine buffers via an acylpyridinium intermediate,^{50,52–54} as is anhydride exchange.^{44,52} Taken together, these factors suggest that the kinetics should be described by the following mechanism:



where Ac is the benzoic acid, An is the anhydride, and Int represents the acylpyridinium intermediate (in eq 1, it is rapidly generated from the *O*-acylisourea, see below). Applying a steady-state approximation in Int (which is not observed) simplifies the scheme with $\alpha = k_3/k_2$. Equation 4 represents background hydrolysis of the EDC, which is expected to be small but significant;²⁹ this reaction was studied independently and k_4 determined to be $7 \times 10^{-3} \text{ min}^{-1}$ under the standard conditions used here. We stress that the rate constants in this treatment are all apparent rate constants, dependent on pD and buffer concentration. The effects of changing these conditions were briefly examined (see below and Supporting Information). However, as our goal was to describe general features of these systems for typical conditions, as opposed to determining already well-understood molecular-level mechanistic details, this dependence was not analyzed in detail.

A typical kinetic run for **An2** is shown in Figure 2a. The solid lines represent the least-squares fit to the kinetic model, with the differential equations describing the mechanism solved numerically (see Supporting Information). Some alternate mechanisms were also

considered: Notably, simplified mechanisms that lack anhydride exchange gave only poor fits, indicating that this aspect is necessary (as is well-known^{44,52}). The addition of other elementary reactions, such as general base catalysis of acylpyridinium hydrolysis by acetate,⁵² did not yield any meaningful improvements to the quality of the fits.

The parameters k_{-2} and α have a strong negative correlation, so care was taken to ensure that sufficient data had been collected that they could be determined with acceptable precision. At least seven runs were performed for each carboxylic acid, varying the starting concentrations of acid ($[\text{Ac}]_0$) and EDC ($[\text{EDC}]_0$). The complete datasets for each system were fit globally. Uncertainties (95% confidence intervals) in the regression were estimated using a nonparametric bootstrapping method.⁶⁵ All fits gave acceptable uncertainties for the parameters. The interdependence of the parameters was then further examined by constructing confidence contour plots, shown in the Supporting Information. This analysis maps out the sum square error for the regression as a function for each pair of k_1 , k_{-2} , and α in order to clearly define the degree to which they can vary while still giving reasonable fits to the experimental data.⁶⁶ The parameters were well-constrained by the data in all cases. We also note that trends in the parameters are consistent with previous work, where applicable, as discussed below.⁶⁷

The substituents in **Ac1**–**Ac4** exert a strong effect on the assembly process, particularly in terms of the maximum anhydride concentrations $[\text{An}]_{\text{max}}$ and the overall time scales of the experiments. Figure 2b shows the behavior of *p*-alkoxy acid **Ac1** and *p*-alkoxycarbonyl acid **Ac4** under comparable conditions. There is a roughly 3-fold difference in $[\text{An}]_{\text{max}}$ and a 50-fold difference in experimental durations (6 h vs <10 min) between them.

The parameters are shown as a function of the Hammett constants σ for each substituent in Figure 3. Notably, the differences in behavior for the four systems (e.g., Figure 2b) are essentially accounted for by variation in k_{-2} ; both the reactions of the acids with EDC (k_1) and the partitioning of the intermediates between anhydride and hydrolysis (α) are invariant within experimental uncertainty. This is in good agreement with the fact that electron

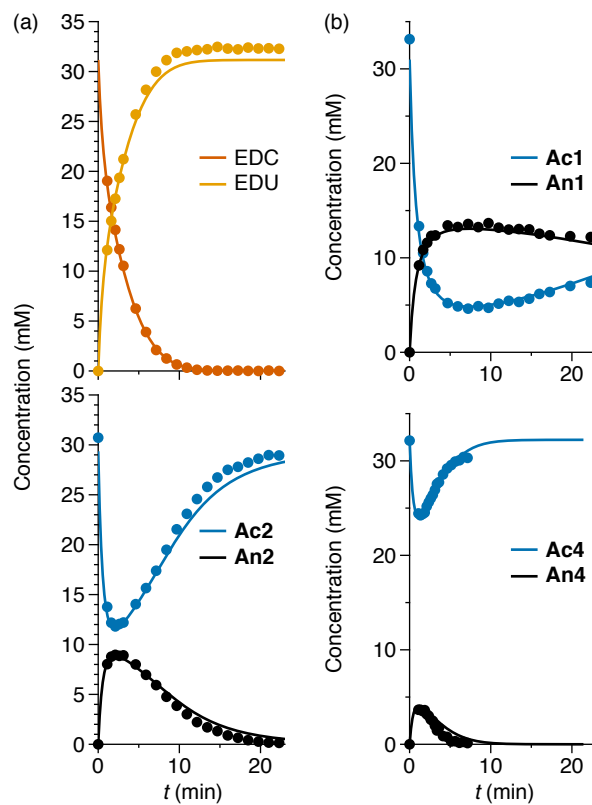


Figure 2: (a) Transient assembly of **An2** (0.5 M pyridine- d_5 buffer, pD 4.5, $I = 1.0$ M (NaCl), D_2O , 298 K). The solid lines represent fits to the model described in the text (note that model is fit to multiple datasets simultaneously, not just the one shown). (b) Formation and hydrolysis of **An1** (top) and **An4** (bottom) on treatment with 1 equiv EDC (EDC consumption and EDU production omitted).

withdrawing groups are well-known to accelerate the hydrolysis of benzoic anhydrides.^{46,68}

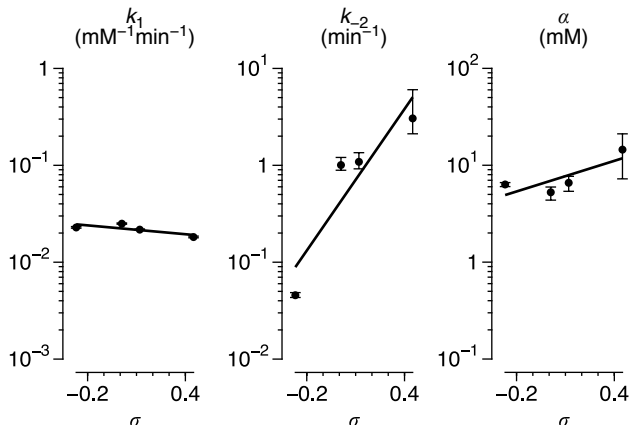


Figure 3: Dependence of kinetic parameters on σ . The uncertainties are 95% confidence intervals based on the global fit to multiple datasets (see Supporting Information).

The effects of changes in pD and buffer concentration were examined for all four systems (see data in the Supporting Information); for **Ac1/An1** it was possible to extract the parameters with reasonable precision from single kinetic runs. As the pD is increased from 4.5 to 5.0 to 5.5 (holding the buffer concentration at 0.5 M), the rate of consumption of EDC decreases for all systems, as does the anhydride lifetime. These behaviors are reflected in the parameters, with a clear decrease in k_1 , increase in k_{-2} , and constant α with increasing pD for the **Ac1/An1** system. Decreasing EDC hydration rate k_1 with increasing pH (around pH 5) is consistent with previous work on the reactivity of EDC, which has shown that the active species for these reactions at acidic/neutral pH is the cyclic ammonioammonium cation (which is less prevalent at higher pH).^{33,39} The anhydride decomposition rate k_{-2} presumably reflects the increasing concentration of free pyridine as the pH increases.⁵² Changing the buffer concentration from 0.4 to 0.5 to 0.6 M (at pD 4.5) gives a corresponding decrease in lifetime. The EDC consumption rate (k_1) is unaffected, confirming that, at these buffer concentrations, initial formation of the *O*-acylisourea is rate-determining followed by rapid formation of the acylpyridinium intermediate. An increase in the observed k_{-2} with increasing buffer concentration, which is required by the mechanism (eq 2), was also observed.

An important characteristic of chemistry for dissipative assembly is that refueling can be used to regenerate the transient state. The response to multiple additions of EDC was studied in the **Ac3**/**An3** system. To begin, a solution of **Ac3** (0.40 mL) was treated with an aliquot of EDC (0.2 mL), as before, and monitored by ^1H NMR spectroscopy. Once the reaction was complete, it was removed from the spectrometer and treated with an additional portion of EDC (the mixture was therefore diluted by 0.20 mL at each step). Three complete refueling cycles were completed as shown in Figure 4. All three experiments were kinetically well-behaved, yielding good fits to the mechanism in eqs 1–4 (solid lines). The lifetimes were comparable in all three cases.

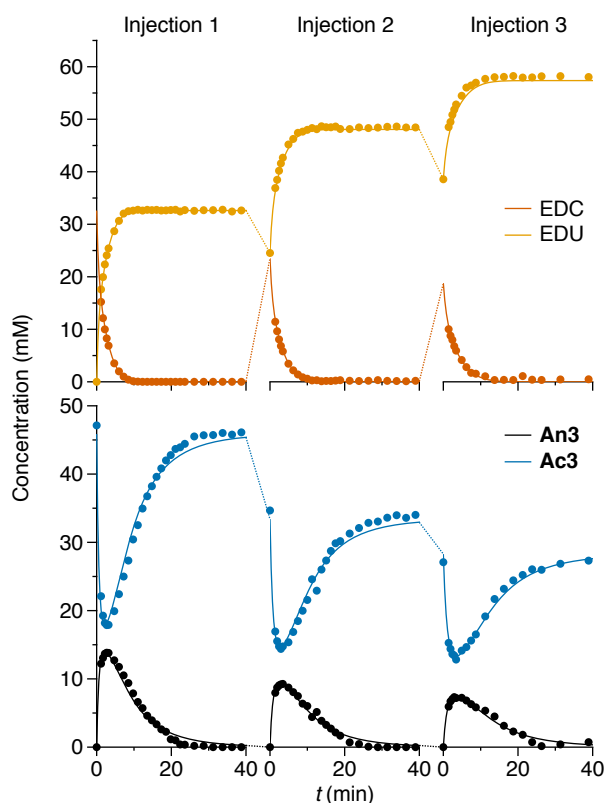


Figure 4: Refueling of the **Ac3**/**An3** system (0.5 M pyridine- d_5 buffer, pD 4.5, $I = 1.0$ M (NaCl), D_2O , 298 K). Note that the mixtures are diluted at each step on addition of EDC (from 0.60 to 0.80 to 1.00 mL), hence the drops in concentration of **Ac3** and EDU at each step.

These reaction conditions allow these systems to be driven by large excesses of EDC. For example, the effect of treating of 45 mM **Ac3** with roughly 9 equiv EDC is shown in Figure

5. Under these conditions, the system remains well-described by the mechanism in eqs 1–4. The system very quickly reaches approximately 90% conversion, with the concentration of **An3** only very slowly decreasing over the course of 10–15 min. As the EDC continues to be consumed, **An3** begins to fall off more quickly. The lifetime of **An3** under these conditions is roughly 30–35 min. This is, of course, longer than a comparable experiment with 1 equiv EDC, but only by about a factor of two, despite the use of almost an order of magnitude more EDC. We did note the appearance of a minor byproduct at the end of the experiment (roughly 3 mM) that did not revert to the starting **Ac3** over the course of several hours (likely an *N*-acylurea).

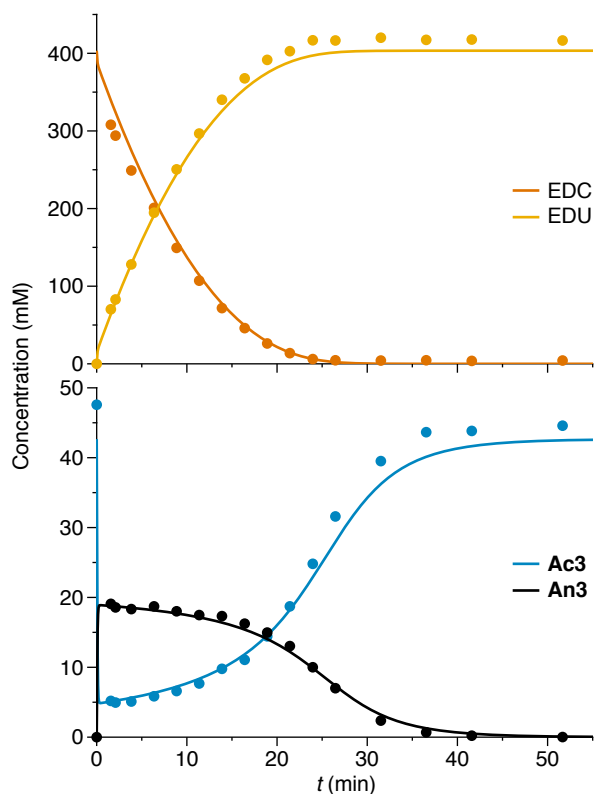


Figure 5: Treatment of **Ac3** with excess (9 equiv) of EDC (0.5 M pyridine- d_5 buffer, pD 4.5, $I = 1.0$ M (NaCl), D_2O , 298 K). Under these conditions a small amount of an unidentified impurity (roughly 3 mM) is apparent in the reaction mixture at the end of the experiment (not shown).

Discussion

The substrate dependence of the chemistry is governed by changes in the kinetic parameters k_1 , k_{-2} , and α , much as modifications in fuel structure affect the rates of dissipative processes.⁶⁹ While each system is, to a first approximation, fully characterized by these parameters, it is useful to identify more-easily appreciated figures of merit. Traditional synthetic reactions are well-described by, for example, yields and reaction times. Of course, the “yields” of transient species generated out-of-equilibrium are zero, by definition, and the experimental time scales are functions of starting conditions for which there are not clear reference values.

The obvious analogue of the yield would be the total quantity of anhydride produced $[\text{An}]_{\text{net}}$ relative to the amount of EDC added $[\text{EDC}]_0$.²⁶ The net anhydride cannot be observed directly; however, it can be calculated for a given set of starting conditions using the parameters for a particular substrate and a mechanistic simulation. For the mechanism in eqs 1–4, it is given by

$$\begin{aligned} [\text{An}]_{\text{net}} &= \int_0^\infty k_1[\text{Ac}][\text{EDC}] \left(1 - \frac{\alpha}{[\text{Ac}] + \alpha}\right) dt \\ &= \int_0^\infty k_{-2}[\text{An}] \left(1 - \frac{[\text{Ac}]}{[\text{Ac}] + \alpha}\right) dt \end{aligned} \tag{5}$$

with the two expressions representing the total anhydride formed or destroyed, respectively. The yield is not 100% because a fraction of the intermediate generated from the EDC (eq 1) simply undergoes hydrolysis (eq 3) rather than giving anhydride and, to a much lesser extent, because of the background EDC hydrolysis (eq 4).

We stress that the overall efficiency as measured by this yield is not obvious from plots of anhydride concentration against time. Take, for example, the behavior of the **Ac1/An1** and **Ac4/An4** systems shown in Figure 2b. They are dramatically different in terms of both time scales and maximum anhydride concentrations. The anhydride yields determined for these two experiments are, however, the same within experimental uncertainty ($59.5^{+0.4}\%$ – 2.4%).

and $64^{+13}_{-17}\%$ for **An1** and **An4**, respectively).

In general, the most intuitive descriptors of the chemistry are functions of the starting conditions. These include the yield, peak anhydride concentration ($[\text{An}]_{\text{max}}$), and lifetime, defined here as the time required for the acid to return to 99% of its starting concentration τ_{99} .⁷⁰ Which characteristics are of interest will be highly application-dependent. For example, for transient assembly, peak anhydride concentration is likely to be important, whereas for the operation of a molecular motor it would not be, strictly speaking, necessary to build up an observable concentration of anhydride at all.

These quantities are easily calculated from simulations of the systems under various starting conditions. Expectations for the treatment of 25 mM solutions of the starting acids ($[\text{Ac}]_0$) with variable amounts of initial EDC ($[\text{EDC}]_0$) are shown in Figure 6. As expected, $[\text{An}]_{\text{max}}$ increases with increasing $[\text{EDC}]_0$, approaching a limit of $[\text{Ac}]_0/2$ (Figure 6a). This limit is reached much more quickly as the anhydride decomposition rate (k_{-2}) decreases (i.e., **Ac1/An1**). Lifetimes τ_{99} increase rapidly with increasing $[\text{EDC}]_0$ but very quickly plateau (Figure 6b), consistent with the results on the use of excess EDC described above (Figure 5). Yields (Figure 6c) approach a limit of $[\text{Ac}]/(\alpha + [\text{Ac}])$ as $[\text{EDC}]_0$ approaches 0.⁷¹ While the limiting yield of **An4** ($63^{+14}_{-9}\%$) appears to be much lower than those of the other acids, this difference is not significant given the uncertainty in our estimate of its α . The yields drop off with increasing $[\text{EDC}]_0$, with the most-pronounced effect for **An1**. This substituent effect derives from the decreasing anhydride hydrolysis rate: production of anhydride from EDC is dependent on the concentration of acid, which, for a given $[\text{EDC}]_0$, is lower throughout a run with **Ac1** as more of it is tied up as slowly decomposing **An1**.

A plot of $[\text{An}]_{\text{max}}$ against yield is shown in Figure 6d. Clearly, there are optimum conditions that balance high conversion against efficiency. For **An1**, **An2**, and **An3**, these conditions correspond to a maximum anhydride concentration of roughly 10 mM (80% conversion) at 70% yield (the difference between **An4** and the others is again not significant within the uncertainties in the parameters).

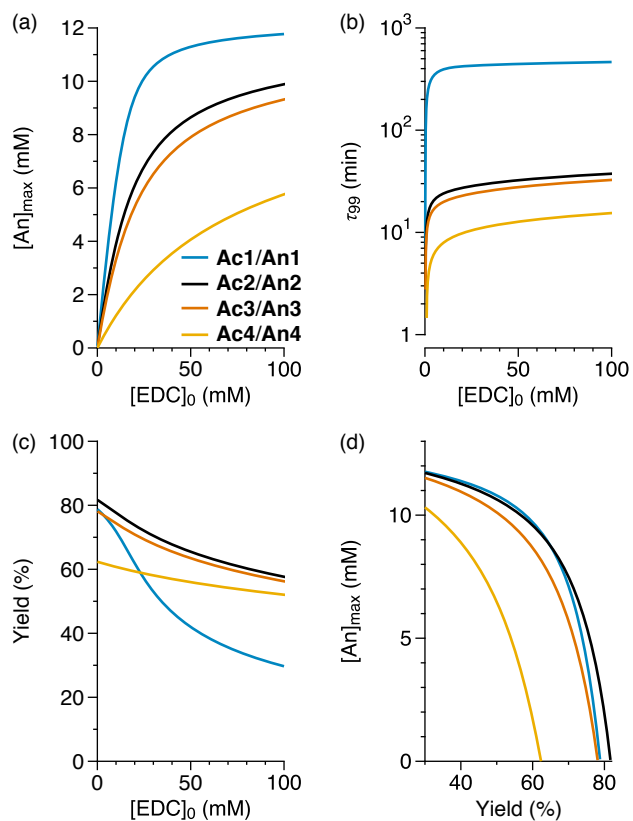


Figure 6: Simulated behavior with variable addition of EDC ($[EDC]_0$) to 25 mM of **Ac1**, **Ac2**, **Ac3**, or **Ac4**. (a) Maximum anhydride concentration $[An]_{max}$ vs $[EDC]_0$. (b) Time to recover 99% of the starting acid τ_{99} vs $[EDC]_0$. (c) Yield (total anhydride produced relative to EDC) vs $[EDC]_0$. (d) $[An]_{max}$ vs yield.

The dependences of $[\text{An}]_{\text{max}}$, τ_{99} , and yield on $[\text{EDC}]_0$ confirm the intuitive picture that, for a system defined by this mechanism, there are diminishing returns in terms of high conversion and time scale for the addition of additional fuel. Even with fairly large excesses of EDC there are small but significant amounts of acid present throughout the experiment (Figure 5). The EDC continues to be consumed but the partitioning of the intermediate (eqs 2 and 3) becomes less productive with decreasing acid concentration. Direct hydrolysis is favored when the concentration of acid falls below α (roughly 10 mM). The plateaus in τ_{99} (Figure 6b) show that the substituent effects on k_{-2} are much more important to determining the overall system lifetime than is the amount of fuel added (at least over reasonable $[\text{EDC}]_0$). Thus, when designing systems that use this chemistry, a poor choice of substrate will not be easily overcome by varying the amount of fuel added.

Much of the value of these results lies in allowing the behavior of new systems to be predicted. That is, the dependence of k_1 , k_{-2} , and α can be used to estimate which substrates represent useful synthetic targets, and which would have too long or short lifetimes or too low anhydride concentrations to be useful. Holding k_1 and α constant at their mean values for all four systems (since they are approximately substituent-independent), the effects of varying k_{-2} on τ_{99} and $[\text{An}]_{\text{max}}$ are shown in Figure 7. For most applications, the range of substituents investigated in this work does a good job of bracketing the region for which the anhydrides would be easily observed (also see Figure 2). Benzoic acids more electron-deficient than **Ac4** would build up only very low concentrations of short-lived anhydrides, whereas acids more electron-rich than **Ac1** would return to equilibrium only very slowly. Of course, it is also possible to further tune rates by varying pD, buffer concentration, solvent makeup, or temperature.

Adding the fuel in a single portion at the beginning of a reaction is convenient for determining mechanistic parameters, but other experimental designs may also be of interest. For example, a constant delivery of fuel can be used to maintain systems in nonequilibrium steady states. This experiment is challenging to monitor, at least using a standard NMR

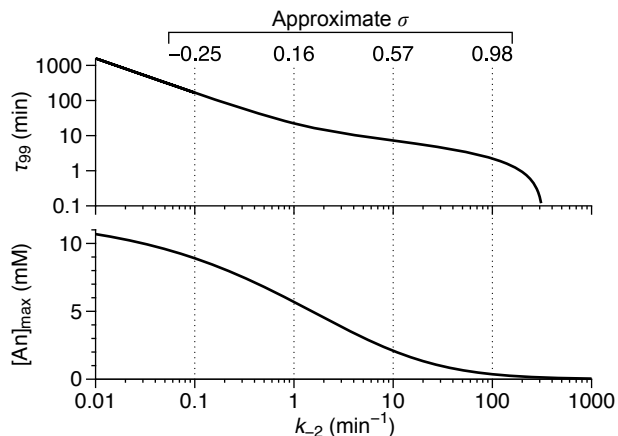


Figure 7: Simulated τ_{99} (top) and $[\text{An}]_{\text{max}}$ (bottom) for variable values of k_{-2} , for $[\text{Ac}]_0 = [\text{EDC}]_0 = 25$ mM. The approximate values of σ corresponding to a given k_{-2} are shown. These were derived from the fit in Figure 3. The curves were calculated by setting k_1 and α to their average values for **An1–An4**.

spectrometer, but is easily simulated using the parameters for each substrate. As shown in Figure 8a, the addition of 5 mM/min of EDC to a 25 mM solution of **Ac2** should give rise to stable concentrations of **Ac2** and **An2**. The steady-state is reached quickly, when less than 2 equiv of fuel has been added ($t = 10$ min). The final concentrations $[\text{An}]_{\text{SS}}$ were calculated as a function of EDC addition rate for all four acids, as shown in Figure 8b. Unsurprisingly, the behavior closely parallels the dependence of $[\text{An}]_{\text{max}}$ on $[\text{EDC}]_0$ (Figure 6a).

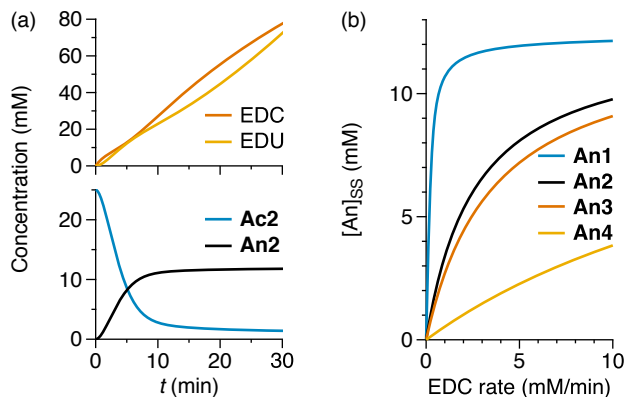


Figure 8: (a) Simulated **Ac2/An2** system with a constant addition of EDC at 5 mM/min to 25 mM **Ac2**. (b) Predicted steady-state concentrations of **An1–An4** as a function of EDC addition rate.

Conclusion

The kinetic parameters describing the EDC-fueled coupling of the series of benzoic acids **Ac1–Ac4** have been determined under typical reaction conditions for nonequilibrium assembly. The experiments are well-behaved, yielding good fits to a simple mechanism, even through multiple refueling cycles or with the addition of large fuel excesses. The acids give markedly different behavior in terms of maximum anhydride concentration ($[\text{An}]_{\text{max}}$) and experimental time scale (τ_{99}), primarily because of differences in the anhydride decomposition rate k_{-2} (which is smaller for electron-rich systems). The overall efficiencies of the reactions, defined as the yields of anhydride relative to the amount of added fuel, can be determined from the experimentally determined parameters at arbitrary starting concentrations of acid and fuel. In general, there are diminishing returns, in terms of maximum anhydride concentration and overall lifetime, as more and more fuel is added, although conditions that come close to maximizing both properties with reasonable fuel quantities can be identified for each substrate. The effects of substrate structure outweigh the effects of adding more fuel, especially for lifetimes. The obtained structure–property relationships should be useful in the design of new systems that exploit this chemistry for nonequilibrium assembly and related processes.

Experimental Section

General

Unless otherwise noted, all starting materials, reagents, and solvents were purchased from commercial sources and used without further purification. Hexa(ethylene glycol) monomethyl ether tosylate (HxGOTs) was synthesized according to a literature procedure.⁷² NMR spectra were measured for CDCl_3 or D_2O solutions at 500 MHz. Chemical shift values (δ) are reported in ppm relative to TMS. The residual CHCl_3 signal was used as an internal stan-

dard for ^1H (7.26 ppm) and the CDCl_3 used for ^{13}C (77.16 ppm). NMR spectra in D_2O were referenced to the acetyl signal of the *N,N*-dimethylacetamide internal standard (2.08 ppm for ^1H , 174.57 ppm for ^{13}C). Melting points were determined using a differential scanning calorimeter at a heating rate of 10 $^\circ\text{C}/\text{min}$.

4-(3,6,9,12,15,18-Hexaoxonadecyloxy)benzoic acid (Ac1)

A mixture of methyl 4-hydroxybenzoate (1.50 g, 9.86 mmol), hexa(ethylene glycol) monomethyl ether tosylate (4.45 g, 9.88 mmol), potassium carbonate (6.82 g, 49.3 mmol), 18-crown-6 (357 mg, 1.35 mmol), and acetone (72 mL) was stirred and heated to reflux for 1 d. The reaction mixture was then cooled to rt and concentrated. Water was added and the mixture extracted with EtOAc (3 \times). The combined organic layers were washed with brine, dried over Na_2SO_4 , filtered, and concentrated. The crude methyl ester intermediate was purified by flash chromatography (5% MeOH in CH_2Cl_2) to afford a yellow oil (2.50 g). This product (2.41 g, 5.60 mmol) was dissolved in a mixture of ethanol and water (1:1 v:v, 62 mL) and treated with KOH (89.6%, 0.880 g, 14.0 mmol). The reaction mixture was stirred and heated to reflux overnight, then cooled to rt and concentrated. It was diluted with water then acidified with 1 M HCl to pH 2. The mixture was extracted with EtOAc (3 \times), and the combined organic extracts washed with brine, dried over Na_2SO_4 , filtered, and concentrated. Purification by flash chromatography (10% MeOH in CH_2Cl_2) gave **Ac1** as a white solid (1.67 g, 42% yield over two steps): mp 42.79 $^\circ\text{C}$; ^1H NMR (500 MHz, CDCl_3) δ 8.04 (d, $J = 9.2$ Hz, 2H), 6.95 (d, $J = 8.7$ Hz, 2H), 4.20 (t, $J = 5.0$ Hz, 2H), 3.88 (t, $J = 5.0$ Hz, 2H), 3.75–3.71 (m, 2H), 3.70–3.61 (m, 16H), 3.56–3.53 (m, 2H), 3.37 (s, 3H); $^{13}\text{C}\{^1\text{H}\}$ NMR (126 MHz, CDCl_3) δ 59.2, 67.8, 69.7, 70.6, 70.69, 70.71, 70.74, 70.8, 71.0, 72.1, 114.5, 122.0, 132.4, 163.3, 171.2; HRMS (ESI-Orbitrap) calcd for $\text{C}_{20}\text{H}_{31}\text{O}_9$ ($[\text{M}-\text{H}]^-$) 415.1968, found 415.1980.

4-(3,6,9,12,15,18-Hexaoxonadecyloxymethyl)benzoic acid (Ac2)

Under an Ar atmosphere, an oven-dried three-necked round-bottomed flask was charged with methyl 4-(hydroxymethyl)benzoate (98%, 2.56 g, 15.1 mmol) and anhydrous DMF (100 mL). Hexa(ethylene glycol) monomethyl ether tosylate (27.2 g, 60.4 mmol) was added as a solution in anhydrous DMF (25 mL). The reaction mixture was stirred, and KHMDS (0.7 M in toluene, 65 mL, 45 mmol) was added dropwise. The reaction mixture was then placed in an oil bath at 70 °C for 5 h. It was then cooled to rt, water was added, and the mixture extracted with Et₂O (3×). The combined organic layers were washed with brine (2×), dried over Na₂SO₄, filtered, and concentrated. The crude methyl ester intermediate was obtained as a yellow oil (6.69 g). A solution of the crude ester (6.69 g) and KOH (2.21 g, 33 mmol) in ethanol:water (1:1 v/v, 170 mL) was heated to reflux overnight. After cooling to rt, the reaction mixture was concentrated to remove the ethanol, then diluted with water. The reaction mixture was acidified with 2 M HCl to pH 2 and extracted with EtOAc (3×). The combined organic layers were washed with brine, dried over Na₂SO₄, filtered, and concentrated. Purification by flash chromatography (4% MeOH in CH₂Cl₂) gave **Ac2** as a yellow oil (0.986 g, 15% yield over two steps): ¹H NMR (500 MHz, CDCl₃) δ 8.03 (d, *J* = 7.8 Hz, 2H), 7.41 (d, *J* = 7.8 Hz, 2H), 4.61 (s, 2H), 3.69–3.66 (m, 2H), 3.66–3.59 (m, 20H), 3.55–3.50 (m, 2H), 3.35 (s, 3H); ¹³C{¹H} NMR (126 MHz, CDCl₃) δ 59.0, 69.9, 70.5, 70.56, 70.58, 70.59, 70.64, 70.7, 71.9, 72.6, 127.3, 128.9, 130.2, 144.3, 170.5; HRMS (ESI-Orbitrap) calcd for C₂₁H₃₃O₉ ([M–H][–]) 429.2125, found 429.2134.

3-(3,6,9,12,15,18-Hexaoxonadecyloxy)benzoic acid (Ac3)

A mixture of methyl 3-hydroxybenzoate (3.07 g, 20.2 mmol), hexa(ethylene glycol) monomethyl ether tosylate (8.89 g, 19.3 mmol), potassium carbonate (13.64 g, 98.69 mmol), 18-crown-6 (700 mg, 2.65 mmol), and acetone (145 mL) was stirred and heated to reflux for 1 d. It was then cooled to rt and concentrated. Water was added and the mixture extracted with EtOAc (3×). The combined organic extracts were washed with brine, dried over Na₂SO₄, filtered,

and concentrated. Purification by flash chromatography (5% MeOH in CH₂Cl₂) gave the methyl ester intermediate as a yellow oil (6.25 g). A solution of the crude ester (6.00 g, 14.0 mmol) in a mixture of EtOH and water (1:1 v/v, 160 mL) was treated with KOH (89.6%, 1.83 g, 29.0 mmol), stirred, and heated to reflux overnight. The reaction mixture was cooled to rt and concentrated to remove the EtOH. It was then acidified with 1 M HCl to pH 2 and extracted with CH₂Cl₂ (3×). The combined organic layers were washed with brine, dried over Na₂SO₄, filtered, and concentrated. Purification by flash chromatography (7% MeOH in CH₂Cl₂) gave **Ac3** as a yellow oil (5.63 g, 73% yield over two steps): ¹H NMR (500 MHz, CDCl₃) δ 7.68 (d, *J* = 7.8 Hz, 1H), 7.63–7.60 (m, 1H), 7.34 (t, *J* = 8.0 Hz, 1H), 7.14 (dd, *J* = 2.3, 8.2 Hz, 1H), 4.18 (t, *J* = 5.0 Hz, 2H), 3.87 (t, *J* = 4.6 Hz, 2H), 3.75–3.70 (m, 2H), 3.70–3.61 (m, 16H), 3.56–3.53 (m, 2H), 3.37 (s, 3H); ¹³C{¹H} NMR (126 MHz, CDCl₃) δ 59.1, 67.8, 69.8, 70.5, 70.6, 70.7, 71.0, 72.0, 115.3, 120.8, 122.8, 129.6, 131.0, 158.9, 170.5; HRMS (ESI-Orbitrap) calcd for C₂₀H₃₁O₉ ([M-H]⁻) 415.1968, found 415.1977.

4-(3,6,9,12,15,18-Hexaoxonadecyloxycarbonyl)benzoic acid (Ac4)

A mixture of terephthalic acid (2.53 g, 15.1 mmol), 4-dimethylaminopyridine (DMAP) (371 mg, 3.04 mmol), hexa(ethylene glycol) monomethyl ether (11.2 g, 37.8 mmol), and CH₂Cl₂ (230 mL) was placed in an ice-water bath. EDC (11.6 g, 74.7 mmol) was added and the reaction mixture stirred for 1 d at rt. It was then concentrated to remove some of the CH₂Cl₂ and washed with 0.2 M HCl. The aqueous layer was extracted with CH₂Cl₂ (2×). The combined organic layers were washed with 0.2 M HCl (2×), water (1×), and brine (2×), then dried over Na₂SO₄, filtered, and concentrated. Purification by flash chromatography (1% NEt₃ and 20% acetone in toluene) gave the diester intermediate as a yellow oil (6.20 g). To a solution of the diester (6.20 g, 8.25 mmol) in water (3 mL) and acetone (3 mL) was added LiOH·H₂O (344 mg, 8.25 mmol) as a solution in water (7.5 mL) and acetone (22.5 mL). The resulting mixture was stirred and heated at reflux overnight. After cooling to rt, the acetone was evaporated and additional water added. The mixture was then washed with

Et₂O (2×). The aqueous layer was acidified with 2 M HCl to pH 2 and extracted with EtOAc (3×). The combined organic layers were washed with brine, dried over Na₂SO₄, filtered, and concentrated. The resulting white solid was suspended in CH₂Cl₂, filtered through Celite, filtered by gravity, and concentrated. Purification by flash chromatography (1% AcOH and 19% CH₂Cl₂ in acetone) gave **Ac4** as a yellow oil (1.14 g, 16% yield over two steps): ¹H NMR (500 MHz, CDCl₃) δ 8.08–8.00 (m, 4H), 4.45 (t, *J* = 5.0 Hz, 2H), 3.81 (t, *J* = 4.6 Hz, 2H), 3.69–3.66 (m, 2H), 3.65–3.56 (m, 16H), 3.52–3.49 (m, 2H), 3.32 (s, 3H); ¹³C{¹H} NMR (126 MHz, CDCl₃) δ 58.9, 64.4, 69.1, 70.3, 70.4, 70.47, 70.50, 70.53, 70.6, 71.8, 129.6, 129.9, 133.8, 134.0, 165.7, 168.7; HRMS (ESI-Orbitrap) calcd for C₂₁H₃₁O₁₀ ([M-H]⁻) 443.1917, found 443.1924.

Reaction monitoring by IR spectroscopy

The benzoic acid (0.20 mmol, 1.0 equiv) was dissolved in distilled water (1.00 mL). EDC (40 mg, 0.21 mmol, 1.0 equiv) was dissolved separately in distilled water (1.00 mL). The two solutions were mixed (*t* = 0) and immediately monitored by IR spectroscopy. FTIR spectra were collected using a micro-Circle cell and TimeBase software. The spectrometer was outfitted with a liquid-nitrogen-cooled mercury cadmium telluride (MCT) detector. A spectrum of distilled water was initially collected and this spectrum was used as the background for all subsequent sample spectra. Approximately 3600 spectra were collected at 4 wavenumber spectral resolution during each experiment using a time interval of 19 seconds.

Reaction monitoring by ¹H NMR spectroscopy

Reaction kinetics were monitored by ¹H NMR spectroscopy at 500 MHz. *N,N*-dimethylacetamide (DMA) was used as an internal standard for the measurement of concentrations, and was also used to calibrate the chemical shift values (δ = 2.08 ppm). Stock solutions (5.00 mL) were prepared in D₂O using the benzoic acid (75 mM, 52 mM, 38 mM, or 19 mM), DMA

(75 mM, 52 mM, 38 mM, or 19 mM), and pyridine- d_5 (600 mM), adjusting the pD with DCl(aq) and bringing the final ionic strengths (I) to 1.0 M using NaCl. Separate solutions of EDC and the appropriate amount of NaCl were prepared in D₂O such that the addition of 200 μ L to 400 μ L of acid solution would deliver the target stoichiometry, maintaining the ionic strength at 1.0 M. The NMR spectrometer was equilibrated at 298 K and locked and shimmed using 600 μ L of a blank (400 μ L of the stock solution and 200 μ L of D₂O). The EDC solution (200 μ L) was added to an NMR tube containing the benzoic acid stock solution (400 μ L) ($t = 0$). The contents were mixed thoroughly by inversion, quickly inserted into the spectrometer, and acquisition started, collecting 1 scan per data point with a delay of 5.00 s and an acquisition time of 2.1825 s.

Supporting Information Available

The Supporting Information is available free of charge on the ACS Publications website at DOI: ...

Additional experiments referred to in the text; description of kinetics analysis and simulation; raw experimental data; NMR spectra of synthesized compounds (PDF)

Program used to fit and model kinetics (ZIP)

Acknowledgement

This work was supported by the U.S. Department of Energy, Office of Science, Basic Energy Sciences, under Award # DE-SC0018645. We also thank Dr. Dominik Konkolewicz for a critical reading of the manuscript.

References

- (1) Mattia, E.; Otto, S. Supramolecular systems chemistry. *Nat. Nanotech.* **2015**, *10*, 111–119.
- (2) Fialkowski, M.; Bishop, K. J. M.; Klajn, R.; Smoukov, S. K.; Campbell, C. J.; Grzybowski, B. A. Principles and implementations of dissipative (dynamic) self-assembly. *J. Phys. Chem. B* **2006**, *110*, 2482–2496.
- (3) van Rossum, S. A. P.; Tena-Solsona, M.; van Esch, J. H.; Eelkema, R.; Boekhoven, J. Dissipative out-of-equilibrium assembly of man-made supramolecular materials. *Chem. Soc. Rev.* **2017**, *46*, 5519–5535.
- (4) Whitesides, G. M.; Grzybowski, B. Self-assembly at all scales. *Science* **2002**, *295*, 2418–2421.
- (5) Dhiman, S.; Sarkar, A.; George, S. J. Bioinspired temporal supramolecular polymerization. *RSC Adv.* **2018**, *8*, 18913–18925.
- (6) Boekhoven, J.; Brizard, A. M.; Kowlgi, K. N. K.; Koper, G. J. M.; Eelkema, R.; van Esch, J. H. Dissipative self-assembly of a molecular gelator by using a chemical fuel. *Angew. Chem., Int. Ed.* **2010**, *49*, 4825–4828.
- (7) Boekhoven, J.; Hendriksen, W. E.; Koper, G. J. M.; Eelkema, R.; van Esch, J. H. Transient assembly of active materials fueled by a chemical reaction. *Science* **2015**, *349*, 1075–1079.
- (8) Debnath, S.; Roy, S.; Ulijn, R. V. Peptide nanofibers with dynamic instability through nonequilibrium biocatalytic assembly. *J. Am. Chem. Soc.* **2013**, *135*, 16789–16792.
- (9) Angulo-Pachón, C. A.; Miravet, J. F. Sucrose-fueled, energy dissipative, transient formation of molecular hydrogels mediated by yeast activity. *Chem. Commun.* **2016**, *52*, 5398–5401.

- (10) Wojciechowski, J. P.; Martin, A. D.; Thordarson, P. Kinetically controlled lifetimes in redox-responsive transient supramolecular hydrogels. *J. Am. Chem. Soc.* **2018**, *140*, 2869–2874.
- (11) Bal, S.; Das, K.; Ahmed, S.; Das, D. Chemically fueled dissipative self-assembly that exploits cooperative catalysis. *Angew. Chem., Int. Ed.* **2019**, *58*, 244–247.
- (12) Maiti, S.; Fortunati, I.; Ferrante, C.; Scrimin, P.; Prins, L. J. Dissipative self-assembly of vesicular nanoreactors. *Nat. Chem.* **2016**, *8*, 725–731.
- (13) Sawczyk, M.; Klajn, R. Out-of-equilibrium aggregates and coatings during seeded growth of metallic nanoparticles. *J. Am. Chem. Soc.* **2017**, *139*, 17973–17978.
- (14) Dambeniaks, A. K.; Vu, P. H. Q.; Fyles, T. M. Dissipative assembly of a membrane transport system. *Chem. Sci.* **2014**, *5*, 3396–3403.
- (15) Sonu, K. P.; Vinikumar, S.; Dhiman, S.; George, S. J.; Eswaramoorthy, M. Bio-inspired temporal regulation of ion-transport in nanochannels. *Nanoscale Adv.* **2019**, *1*, 1847–1852.
- (16) Wilson, M. R.; Solà, J.; Carlone, A.; Goldup, S. M.; Lebrasseur, N.; Leigh, D. A. An autonomous chemically fuelled small-molecule motor. *Nature* **2016**, *534*, 235–240.
- (17) Wood, C. S.; Browne, C.; Wood, D. M.; Nitschke, J. R. Fuel-controlled reassembly of metal–organic architectures. *ACS Cent. Sci.* **2015**, *1*, 504–509.
- (18) Del Grosso, E.; Amodio, A.; Ragazzon, G.; Prins, L. J.; Ricci, F. Dissipative synthetic DNA-based receptors for the transient loading and release of molecular cargo. *Angew. Chem., Int. Ed.* **2018**, *57*, 10489–10493.
- (19) Wang, G.; Tang, B.; Liu, Y.; Gao, Q.; Wang, Z.; Zhang, X. The fabrication of a supra-amphiphile for dissipative self-assembly. *Chem. Sci.* **2016**, *7*, 1151–1155.

- (20) Wang, G.; Sun, J.; An, L.; Liu, S. Fuel-driven dissipative self-assembly of a supra-
amphiphile in batch reactor. *Biomacromolecules* **2018**, *19*, 2542–2548.
- (21) Tena-Solsona, M.; Rieß, B.; Grötsch, R. K.; Löhrer, F. C.; Wanzke, C.; Käs Dorf, B.;
Bausch, A. R.; Müller-Buschbaum, P.; Lieleg, O.; Boekhoven, J. Non-equilibrium dissi-
pative supramolecular materials with a tunable lifetime. *Nat. Commun.* **2017**, *8*, 15895.
- (22) Tena-Solsona, M.; Wanzke, C.; Riess, B.; Bausch, A. R.; Boekhoven, J. Self-selection of
dissipative assemblies driven by primitive chemical reaction networks. *Nat. Commun.*
2018, *9*, 2044.
- (23) Grötsch, R. K.; Angi, A.; Mideksa, Y. G.; Wanzke, C.; Tena-Solsona, M.; Feige, M. J.;
Rieger, B.; Boekhoven, J. Dissipative self-assembly of photoluminescent silicon
nanocrystals. *Angew. Chem., Int. Ed.* **2018**, *57*, 14608–14612.
- (24) Rieß, B.; Wanzke, C.; Tena-Solsona, M.; Grötsch, R. K.; Maity, C.; Boekhoven, J.
Dissipative assemblies that inhibit their deactivation. *Soft Matter* **2018**, *14*, 4852–4859.
- (25) Rieß, B.; Boekhoven, J. Applications of dissipative supramolecular materials with a
tunable lifetime. *ChemNanoMat* **2018**, *4*, 710–719.
- (26) Kariyawasam, L. S.; Hartley, C. S. Dissipative assembly of aqueous carboxylic acid
anhydrides fueled by carbodiimides. *J. Am. Chem. Soc.* **2017**, *139*, 11949–11955.
- (27) Zhang, B.; Jayalath, I. M.; Ke, J.; Sparks, J. L.; Hartley, C. S.; Konkolewicz, D.
Chemically fueled covalent crosslinking of polymer materials. *Chem. Commun.* **2019**,
55, 2086–2089.
- (28) Díaz Pérez, V. M.; Ortiz Mellet, C.; Fuentes, J.; García Fernández, J. M. Synthesis
of glycosyl(thio)ureido sugars via carbodiimides and their conformational behaviour in
water. *Carbohydr. Res.* **2000**, *326*, 161–175.

- (29) Nakajima, N.; Ikada, Y. Mechanism of amide formation by carbodiimide for bioconjugation in aqueous media. *Bioconjugate Chem.* **1995**, *6*, 123–130.
- (30) Astumian, R. D. Stochastic pumping of non-equilibrium steady-states: how molecules adapt to a fluctuating environment. *Chem. Commun.* **2018**, *54*, 427–444.
- (31) Whitesides, G. M.; Mathias, J. P.; Seto, C. T. Molecular self-assembly and nanochemistry: a chemical strategy for the synthesis of nanostructures. *Science* **1991**, *254*, 1312–1319.
- (32) Khorana, H. G. The chemistry of carbodiimides. *Chem. Rev.* **1953**, *53*, 145–166.
- (33) Ibrahim, I. T.; Williams, A. Reaction of the water-soluble reagent *N*-ethyl-*N'*-(3-dimethylaminopropyl)carbodiimide with nucleophiles: participation of the tautomeric cyclic ammonioamidine as a kinetically important intermediate. *J. Am. Chem. Soc.* **1978**, *100*, 7420–7421.
- (34) Ibrahim, I. T.; Williams, A. Concerted general acid catalysis in the reaction of acetate ion with water-soluble carbodi-imide. *J. Chem. Soc., Chem. Commun.* **1980**, 25–27.
- (35) Ibrahim, I. T.; Williams, A. Direct spectrophotometric observation of an *O*-acylisourea intermediate: concerted general acid catalysis in the reaction of acetate ion with a water-soluble carbodi-imide. *J. Chem. Soc., Perkin Trans. 2* **1982**, 1459–1466.
- (36) DeTar, D. F.; Silverstein, R. Reactions of carbodiimides. I. The mechanisms of the reactions of acetic acid with dicyclohexylcarbodiimide. *J. Am. Chem. Soc.* **1966**, *88*, 1013–1019.
- (37) Khorana, H. G. Peptides. Part III. Selective degradation from the carboxyl end. The use of carbodi-imides. *J. Chem. Soc.* **1952**, 2081–2088.
- (38) Mikolajczyk, M.; Kielbasinski, P. Recent developments in the carbodiimide chemistry. *Tetrahedron* **1981**, *37*, 233–284.

- (39) Williams, A.; Ibrahim, I. T. A new mechanism involving cyclic tautomers for the reaction with nucleophiles of the water-soluble peptide coupling reagent 1-ethyl-3-(3'-(dimethylamino)propyl)carbodiimide (EDC). *J. Am. Chem. Soc.* **1981**, *103*, 7090–7095.
- (40) Williams, A.; Ibrahim, I. T. Carbodiimide chemistry: recent advances. *Chem. Rev.* **1981**, *81*, 589–636.
- (41) Iwasawa, T.; Wash, P.; Gibson, C.; Rebek Jr, J. Reaction of an introverted carboxylic acid with carbodiimide. *Tetrahedron* **2007**, *63*, 6506–6511.
- (42) DeTar, D. F.; Silverstein, R. Reactions of carbodiimides. II. The reactions of dicyclohexylcarbodiimide with carboxylic acids in the presence of amines and phenols. *J. Am. Chem. Soc.* **1966**, *88*, 1020–1023.
- (43) Balcom, B. J.; Petersen, N. O. Solvent dependence of carboxylic acid condensations with dicyclohexylcarbodiimide. *J. Org. Chem.* **1989**, *54*, 1922–1927.
- (44) Bunton, C. A.; Fuller, N. A.; Perry, S. G.; Shiner, V. J. The pyridine catalysed hydrolysis of carboxylic anhydrides. *Tetrahedron Lett.* **1961**, *2*, 458–460.
- (45) Bunton, C. A.; Fendler, J. H. The hydrolysis of carboxylic anhydrides. VII. Electrolyte effects on the acid hydrolysis. *J. Org. Chem.* **1966**, *31*, 3764–3771.
- (46) Berliner, E.; Altschul, L. H. The hydrolysis of substituted benzoic anhydrides. *J. Am. Chem. Soc.* **1952**, *74*, 4110–4113.
- (47) Brandão, T. A. S.; Dal Magro, J.; Chiaradia, L. D.; da Graça Nascimento, M.; Nome, F.; Tato, J. V.; Yunes, R. A. Catalytic and inhibitory effects of β -cyclodextrin on the hydrolysis of benzoic anhydride. *J. Phys. Org. Chem.* **2004**, *17*, 370–375.
- (48) Bafna, S. L.; Gold, V. The hydrolysis of acetic anhydride. Part II. Catalysis by pyridine. *J. Chem. Soc.* **1953**, 1406–1409.

- (49) Bunton, C. A.; Perry, S. G. The acid-catalysed hydrolysis of carboxylic anhydrides. *J. Chem. Soc.* **1960**, 3070–3079.
- (50) Butler, A. R.; Gold, V. 859. The hydrolysis of acetic anhydride. Part VII. Catalysis by pyridine and methylpyridines in acetate buffers. *J. Chem. Soc.* **1961**, 4362–4367.
- (51) Calvaruso, G.; Cavasino, F. P.; Di Dio, E. Kinetics of the hydrochloric acid-catalysed hydrolyses of benzoic anhydrides in various dioxan–water mixtures. *J. Chem. Soc., Perkin Trans. 2* **1976**, 993–995.
- (52) Fersht, A. R.; Jencks, W. P. The acetylpyridinium ion intermediate in pyridine-catalyzed hydrolysis and acyl transfer reactions of acetic anhydride. Observation, kinetics, structure-reactivity correlations, and effects of concentrated salt solutions. *J. Am. Chem. Soc.* **1970**, *92*, 5432–5442.
- (53) Johnson, S. L. Hydrolysis of acetic anhydride in the presence of acetate buffer and pyridine. *J. Phys. Chem.* **1963**, *67*, 495–496.
- (54) Koskikallio, J. The kinetics of the base-catalysed hydrolysis of acetic anhydride in dioxane-water mixtures. *Acta Chem. Scand.* **1963**, *17*, 1417–1425.
- (55) By “typical conditions”, we mean a straightforward set of conditions that should serve as a useful starting point for carbodiimide-fueled systems.
- (56) A preprint of this manuscript was deposited in ChemRxiv, doi: 10.26434/chemrxiv.9941627.
- (57) Hansch, C.; Leo, A.; Taft, R. W. A survey of Hammett substituent constants and resonance and field parameters. *Chem. Rev.* **1991**, *91*, 165–195.
- (58) Ramazani, A.; Nasrabadi, F. Z.; Rezaei, A.; Rouhani, M.; Ahankar, H.; Asiabi, P. A.; Joo, S. W.; Ślepokura, K.; Lis, T. Synthesis of *N*-acylurea derivatives from carboxylic

- acids and *N,N'*-dialkyl carbodiimides in water. *J. Chem. Sci. (Berlin, Ger.)* **2015**, *127*, 2269–2282.
- (59) Hegarty, A. F.; McCormack, M. T.; Brady, K.; Ferguson, G.; Roberts, P. J. Competing acyl transfer and intramolecular O→N acyl group migration from an isolable *O*-acylisourea. *J. Chem. Soc., Perkin Trans. 2* **1980**, 867–875.
- (60) ¹³C NMR spectroscopy was used because its wide chemical shift range, relative insensitivity of chemical shifts to matrix effects, and larger number of signals makes comparisons more convincing than those of ¹H NMR spectra.
- (61) There is also a subtle, but significant, concentration dependence of the chemical shifts of **Ac2**, which accounts for most of the discrepancy between the chemical shifts in the blank vs the kinetic runs. The remainder likely results from differences in mixture composition (ionic strength, presence of EDC/EDU).
- (62) The anhydrides are presumed to be dimers, as opposed to supramolecular polymers, because the total changes in chemical shifts are < 1 ppm (ref. 63).
- (63) Martin, R. B. Comparisons of indefinite self-association models. *Chem. Rev.* **1996**, *96*, 3043–3064.
- (64) Neises, B.; Steglich, W. Simple method for the esterification of carboxylic acids. *Angew. Chem., Int. Ed. Engl.* **1978**, *17*, 522–524.
- (65) Fox, J. *Applied Regression Analysis and Generalized Linear Models*, 3rd ed.; Sage Publishing: New York, 2016; Chapter 21, pp 587–606.
- (66) Johnson, K. A.; Simpson, Z. B.; Blom, T. FitSpace Explorer: An algorithm to evaluate multidimensional parameter space in fitting kinetic data. *Anal. Biochem.* **2009**, *387*, 30–41.

- (67) For **An1**, it was possible to analyze the hydrolysis (eqs 2 and 3) independently by including only datapoints following the complete consumption of EDC. Doing so yields values of k_{-2} and α of 0.05 and 6, in agreement with the results for the complete mechanism.
- (68) The slope gives a reaction constant (ρ) of +2.4; of course, with 4 points we cannot say with certainty that the dependence is linear.
- (69) Biagini, C.; Albano, S.; Caruso, R.; Mandolini, L.; Berrocal, J. A.; Di Stefano, S. Variations in the fuel structure control the rate of the back and forth motions of a chemically fuelled molecular switch. *Chem. Sci.* **2018**, *9*, 181–188.
- (70) The choice of 99% recovery as the definition of lifetime is, of course, arbitrary. Using a relatively high threshold defines τ as a near-complete reset of the system. It also allows the behavior of systems with relatively little EDC to be considered (i.e., if only 75% were used as the threshold, only systems with sufficient EDC to consume 25% of the acid would have meaningful lifetimes).
- (71) Strictly speaking, the limiting yield is only exactly $[\text{Ac}]/(\alpha + [\text{Ac}])$ in the absence of background EDC hydrolysis (eq 4).
- (72) Meiners, F.; Ross, J. H.; Brand, I.; Buling, A.; Neumann, M.; Köster, P. J.; Christoffers, J.; Wittstock, G. Modification of silicon oxide surfaces by monolayers of an oligoethylene glycol-terminated perfluoroalkyl silane. *Colloids Surf., A* **2014**, *449*, 31–41.

Graphical TOC Entry

